EUROFUSION WPMAT-PR(15) 14629

M Chiapetto et al.

Simulation of nanostructural evolution under irradiation in Fe-9%Cr-C alloys: an object kinetic Monte Carlo study of the effect of temperature and dose-rate

Preprint of Paper to be submitted for publication in
Nuclear Materials and Energy

This work has been carried out within the framework of the EUROfusion Consortium and has received funding from the Euratom research and training programme 2014-2018 under grant agreement No 633053. The views and opinions expressed herein do not necessarily reflect those of the European Commission.

Simulation of nanostructural evolution under irradiation in Fe-9%Cr-C alloys: an object kinetic Monte Carlo study of the effect of temperature and dose-rate

M. Chiapetto[a,b,1], C.S. Becquart[b], L. Malerba[a]

[a]*SCK•CEN, Nuclear Materials Science Institute, Boeretang 200, B-2400 Mol, Belgium*
[b]*Unité Matériaux Et Transformations (UMET), UMR 8207, Université de Lille 1, ENSCL, F-59600 Villeneuve d'Ascq Cedex, France*

Abstract

This work explores the effects of both temperature and dose-rate on the nanostructural evolution under irradiation of the Fe-9%Cr-C alloy, model material for high-Cr ferritic/martensitic steels. Starting from an object kinetic Monte Carlo model validated at 563 K, we investigate here the accumulation of radiation damage as a function of temperature and dose-rate, attempting to highlight its connection with low-temperature radiation-induced hardening. The results show that the defect cluster mobility becomes high enough to partially counteract the material hardening process only above ~290°C, while high fluxes are responsible for higher densities of defects, so that an increase of the hardening process with increasing dose-rates may be expected.

Keywords: OKMC; object kinetic Monte Carlo; martensitic alloys; Fe-Cr-C; neutron irradiation; dose-rate; irradiation temperature.

1. Introduction

High-chromium ferritic/martensitic (F/M) steels are regarded as the main candidate structural material for the breeding blanket of future fusion reactors [1], as well as, in a medium-term perspective, for fuel cladding and other core components in GenIV reactors [2,3]. The reason for this choice is that, in addition to enabling the long-term activation to be minimized by choosing appropriate alloying elements, they present superior thermal and mechanical properties as compared to austenitic steels, such as higher resistance to radiation-induced swelling [4-6]. However, they also exhibit low-temperature irradiation hardening and embrittlement: even though the choice of 9%Cr was made to minimize this effect [7], it may make their use problematic at temperatures below 400°C [5]. Both hardening and embrittlement in irradiated materials are believed to be due to the accumulation of radiation damage: the flux of fast neutrons impinging on the metal leaves behind a large amount of point-defects that, throughout the irradiation process, can migrate and interact with each other, forming voids and dislocation loops, while interacting with pre-existing features inside the material, like dislocation lines, grain boundaries and solute atoms, leading to segregation and precipitation processes. The influence of Cr content, together with that of different environmental variables such as irradiation temperature and dose-rate, are known to have an important influence on the nanostructural evolution under neutron irradiation of F/M steels. Unfortunately, no fully exhaustive record of irradiation campaigns on F/M steels neutron-irradiated at different temperatures and dose-rates exists, due to the difficulty and cost of obtaining such a variety of conditions in existing facilities. Computer simulation models offer in this context an effective and inexpensive way to explore the effect of these parameters and try to understand the degradation processes that occur in these materials.

In this work, using a validated object kinetic Monte Carlo (OKMC) model for neutron irradiated Fe-Cr-C alloys [8], we studied the effect of both irradiation temperature and dose-rate on the Fe-9%Cr-C model alloy. This was done with a twofold purpose: first, to test the validity of the model outside its range of calibration (i.e. 563 K and 10^{-7} dpa/s [9]) and, secondly, assuming reasonable validity of the model, to try to make conclusions on the not yet fully predictable dependence of the defect cluster nanostructural evolution upon external variables like irradiation temperature and dose-rate in F/M steels. The paper is organized as follows: the OKMC method adopted is succinctly presented in section 2, together with the main aspects of our parameterization. Section 3 shows the results of our investigation, while in section 4 an overview on the state-of-the-art comprehension of the variables investigated on the nanostructural behavior of irradiated F/M alloys is reported and analogies with our results are outlined. Finally, section 5 contains our conclusions.

2. Method and parameterization

For all our simulations we used the OKMC code LAKIMOCA, thoroughly described in [10]. The approach we adopted is explained in detail in [8,11,12]. For convenience, we highlight here the fundamental ideas. The OKMC is a stochastic method used to describe the evolution of defects and their clusters in materials subjected to irradiation, disregarding the detail of processes directly involving atoms and focusing instead only on the properties of defects, treated as objects. Neutron irradiation produces point defects, namely vacancies (V) and self-interstitial atoms (SIA), which may form clusters. The objects we consider are therefore V and SIA clusters or any other nanostructural feature that needs to be included, like carbon (C) atoms or carbon-vacancy (C_2V, see [11]) complexes. All objects are located in a simulation volume in which their coordinates are known and tracked. Specifically, in our model C atoms and C_2V complexes act as immobile spherical traps for mobile defects (V and SIA clusters), and are characterized by a certain binding energy, E_t, depending on the size and type of the trapped object.

[1] Corresponding author. Tel.: +32-14-333181.
E-mail address: mchiapet@sckcen.be.

It is important to note that Cr atoms are not introduced explicitly in our model, but their presence is reflected in the change of the mobility of SIA objects, i.e. applying a "grey alloy" approach (see [8] for further details). This choice was dictated by the need to avoid the introduction of an unnecessarily large number of objects in the system, that would have slowed down enormously our simulations.

Every object introduced in the system has an associated spherical reaction volume, with the exception of large dislocation loops (>150 SIA) which are represented by toroids, and can undergo events such as migration, recombination, or clustering of defects, which take place in the simulation volume according to pre-defined probabilities given in terms of Arrhenius frequencies for thermally activated processes:

$$\Gamma_i = \nu_i \exp\left(\frac{-A_i}{k_B T}\right) \qquad (1)$$

Here ν_i is the attempt frequency (alias the prefactor) of the event i; A_i is the corresponding activation energy, which must embody both the thermodynamics and the kinetics of the system being studied; k_B is the Boltzmann's constant and T is the irradiation temperature expressed in K. For every simulation step, among all the possible events, one and only one is chosen, based on the corresponding probabilities defined by the parameterization and according to the stochastic Monte Carlo algorithm [13]. Time elapses according to the residence time algorithm [14]:

$$\Delta t \propto \frac{1}{\Sigma_1^N \Gamma_i} \qquad (2)$$

where the time increase is obtained as inverse of the sum of all the frequencies Γ_i associated with each of the N possible events.

When LAKIMOCA simulates the damage production from neutron irradiation, debris of displacement cascades (containing V and SIA objects of different sizes) are introduced in the system taking them randomly from a database [15-17] previously obtained using molecular dynamics. Residual Frenkel pairs are also introduced [18]. The impinging neutron flux is thus transformed into a defect production rate: number of introduced defects per unit time and volume, directly corresponding to a certain dpa rate. The displacement cascades range over different energies (5 keV, 10 keV, 20 keV, … , 100 keV) and the accumulated dpa is calculated using the NRT formula [13].

In the model, grain boundaries act as a spherical surface sink for defect clusters of all sizes. The absorption of defects is taken into account by applying the algorithm described in [19]: each object has two sets of coordinates, one, subjected to periodic boundary conditions, that expresses its position in the simulation box, and a second one, not subjected to periodicity, that expresses its distance from the centre of a supposedly spherical grain (randomly initialized when the object is created). When the latter distance happens to correspond to the grain radius, the objects disappear, irrespective of their position inside the box. The grain size for the Fe-9%Cr-C model alloy used as reference is 20 μm [20]. A second kind of sinks in irradiated materials are dislocations, which are reproduced here by spherical sinks randomly distributed in the simulation volume: their number and size are chosen in such a way that the sink strength associated with them equals the corresponding material dislocation density [8,21]. The dislocation density of the reference Fe-9%Cr-C model alloys was reported to be 6.3×10^{13} m^{-2} [22]. However, since SIA clusters are often observed by transmission electron microscopy to decorate dislocations in the alloys of interest here [22-24], meaning that they are not absorbed if large enough, we only allow defect clusters smaller than the core of dislocations, i.e. size 1-4, to be absorbed by the spherical sinks: the latter are transparent to bigger defect clusters. Finally, the C concentration in the matrix, which also determines the concentration of traps for point defect clusters, was assumed to be 20 appm, based on experimental indications [8,25]. All other parameters were chosen to be exactly the same as in [8].

All simulations were performed in a non-cubic box of size 600×750×1000 a_0^3 ($a_0 = 2.87\times10^{-10}$ m is the lattice parameter of α-Fe) in order to avoid potential anomalies from 1D-migrating SIA clusters bigger than ~5 defects entering a migration trajectory loop, as discussed in [26], due to the periodic boundary conditions which were applied in all three directions.

3. Results

3.1. Effect of irradiation temperature

Fig. 1 shows the evolution with irradiation temperature of both SIA and V cluster population number densities (upper and lower left) and mean sizes (upper and lower right). All simulation results are reported at 0.6 dpa. The lower temperature range analysed here is relevant for the water-cooled design of DEMO, while the upper bound of 350°C was dictated by simulation time limits.

SIA loops that are big enough to be seen in the transmission electron microscope (TEM), i.e. with a radius larger than ~1.3 nm, and SIA clusters containing between 10 and 90 SIA, i.e. corresponding to sizes below the TEM visibility threshold, have been reported separately. By increasing the irradiation temperature, the number density of bigger SIA clusters decreases by almost two orders of magnitude when going from 250 to 350°C, while the number density of SIA defects non visible in TEM in the same temperature range decreases only by about one order of magnitude. At the same time, the mean size of this TEM-invisible population remains almost constant, while the average size of TEM-visible SIA clusters decreases by a factor two when the irradiation temperature increases from 270 to 330°C. According to our OKMC model the number density decrease of the SIA cluster population can be ascribed to an increase of about 40% in the number of defects absorbed by sinks (i.e. dislocations and grain boundaries) at 350°C when compared to the lowest irradiation temperature; at the same time, the lower mean size of TEM-visible SIA loops is a combined consequence of major loss of defects at sinks and increase of around 3% in the amount of recombinations at 350°C.

The total amount of vacancies that is left in the system after irradiation is also seen to gradually decrease with increasing irradiation temperatures: this trend is further enhanced in the case of vacancy clusters bigger than ~1 nm (i.e. more than 45 vacancy per cluster), which are seen not to form any more already above ~310°C, meaning that the density to be expected in reality falls

below 10^{20} m^{-3}. At 310°C the number of recombinations predicted by our OKMC code, always at 0.6 dpa, had increased by about 3.5%, while even more important was the increase in the number of vacancy objects that had been absorbed by sinks (more than five times more than at 250°C). Vacancy clustering was also boosted by around 20% when moving from 250 to 310°C, making the void mean size increase by almost a factor 4 in that range of temperatures. As a matter of fact, small and medium size vacancy clusters become thermally unstable in the higher temperature range and are thus more likely to release highly mobile (more mobile than clusters) single-vacancies which can, on the one side, erode the interstitial-type defect population and, on the other, increase the dimensions of the limited number of larger voids. The origin of the defect clusters behaviour observed here is that, as has been presented in section 2, the probabilities of mechanisms such as defect migration or emission of a single-vacancy from a bigger cluster are ruled by an Arrhenius dependence with the system temperature (Eq. 1): thus, the higher the irradiation temperature, the higher the probability for these events to take place.

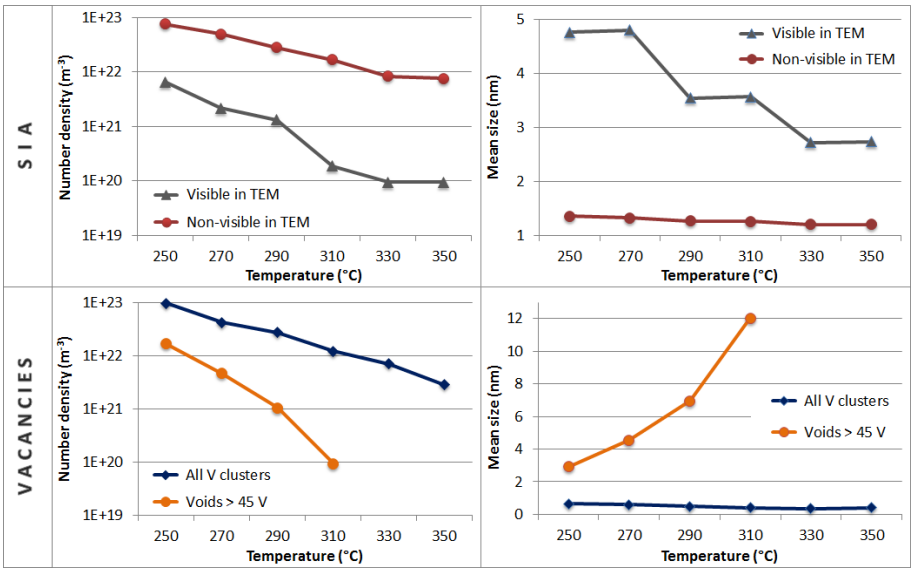

Fig. 1. Number density and mean size evolution with irradiation temperature of both SIA (above) and V (below) cluster populations at 0.6 dpa.

3.2. Study on the impact of dose-rate

The evolution of both SIA and V cluster population number densities (upper and lower left) and mean sizes (upper and lower right), neutron irradiated with increasing dose-rates, are shown in Fig. 2. All simulation results are reported at 0.2 dpa. The values of dose-rates were chosen in order to cover a wide range, going from dose-rates typical of surveillance programmes in light water reactors (~10^{-9} dpa/s), to rates characteristic of irradiation in materials test reactors (MTR), as well as first wall fusion systems (~10^{-7}-10^{-6} dpa/s), up to values close to those reached under ion irradiation (~10^{-3} dpa/s), which in reality are unattainable with neutrons.
As in section 3.1, when analyzing the simulation results the SIA cluster population was divided into two groups: SIA loops that are visible in TEM and SIA clusters corresponding to sizes below the TEM visibility threshold. Our OKMC model predicted an increase in the number densities of both TEM-visible and -invisible SIA defects with increasing dose-rates: this increase was more pronounced in the case of bigger loops (more than three orders of magnitude difference between the lowest and the highest dose-rate), while the number densities of the two classes of SIA defect clusters converged towards the same value at 10^{-3} dpa/s. The reason for this effect is that, with increasing dose-rate, the number of absorptions at sinks decreases by almost two orders of magnitude, which is close to the difference in number density between TEM-invisible and -visible SIA defects after irradiation at 10^{-9} dpa/s: the amount of small SIA defects absorbed at the lower dose-rates constitutes possible nucleation points for TEM-invisible SIA clusters at higher fluxes. The mean size of TEM-visible SIA clusters remained almost constant for all the investigated flux values, while the mean size of smaller SIA clusters was seen to increase slightly: since the number density of the latter stabilizes above ~10^{-7} dpa/s, a redistribution in size towards bigger SIA clusters (though still below TEM-resolution) clearly occurred at the higher dose-rates.

The number density of the vacancy cluster population was also predicted to increase by about three orders of magnitude between the lower and the higher dose-rate, while no voids were observed after irradiation up to 0.2 dpa at the lowest neutron flux, meaning that clusters did not manage to grow to sufficient size. Indeed, the mean size of bigger voids decreased sharply with increasing dose-rate. The reason for the results obtained lies in the fact that at lower dose-rate a smaller density of defects are introduced per unit volume and unit time, thus the interaction between radiation induced defects occur less frequently. This results in a smaller density of defect nucleation points (e.g. vacancy clusters), with a larger number of defects migrating to each point, leading to growth; the opposite becomes true when the dose rate increases. The total number of recombinations, always at 0.2 dpa, was found to decrease by about 10% when moving from a dose-rate of 10^{-9} dpa/s to 10^{-3} dpa/s, thereby explaining the increase in number density observed, while vacancy clustering was also seen to decrease by around 40%.

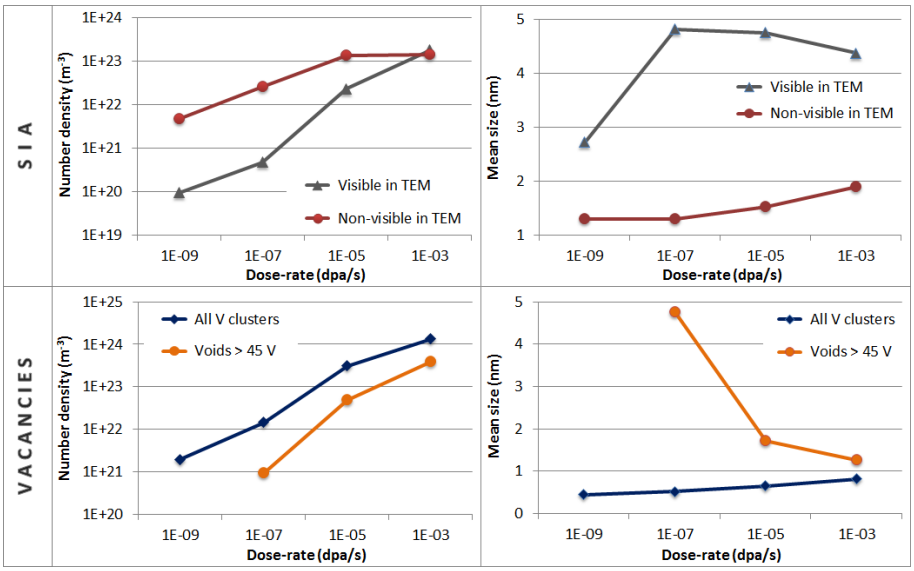

Fig. 2. Number density and mean size evolution with dose-rate of both SIA (above) and V (below) cluster populations at 0.2 dpa.

4. Discussion

In the literature there is no record of Fe-Cr alloys or F/M steels neutron irradiated under a variety of temperatures and dose-rates conditions similar to those studied here: a direct comparison between our OKMC simulation results and experimental observations on irradiated materials is thus not possible and only trends can be compared, with some caution about whether or not the real irradiation conditions are reproduced by the model.

The simulation results concerning visible SIA loops can be compared with trends observed in TEM studies of alloys of this type; those concerning vacancies may be compared with positron annihilation spectroscopy (PAS) analysis in the case of small vacancy clusters and TEM studies for the void population. More difficult is to make conclusions about trends in the case of the population of TEM-invisible SIA clusters. Small SIA clusters below TEM resolution may be assumed to be associated with the high density of small NiSiPCr-rich solute clusters identified by atom probe tomography (APT) in neutron irradiated Fe-Cr alloys [8,27]: the leading idea is that these solutes may heterogeneously nucleate on small SIA loops. This assumption is supported by the fact that atomistic simulations have clearly shown that Cr tends to segregate on dislocation loops [28] and that other solutes follow the same trend, in particular Ni, Mn and Cu [29]. There is also unambiguous experimental evidence of segregation of Cr and other solutes (Si, Ni, Cu, …) on loops in F/M steels from energy-dispersive X-ray spectroscopy studies and also APT studies, e.g. [30] and, more recently, [31]. Furthermore, in [27] it was also verified that NiSiPCr clusters had an orientation compatible with the habit planes of the dislocation loops typical for bcc Fe based alloys, i.e. {111} and {110}. Consistently, the number density of TEM-invisible loops predicted by the OKMC model at ~300°C and 10^{-7} dpa/s was found to be of the same order of magnitude as the number density of solute clusters found in APT experiments under corresponding irradiation conditions [8]. We therefore consider here that the concentration of SIA clusters below TEM resolution is roughly the concentration of the small NiSiPCr-rich solute clusters seen in APT. However, since we applied a "grey alloy" approach, where solute atoms are not explicitly included, we can only verify whether the number density of TEM-invisible loops in our simulations is of the same order of magnitude as the number density of solute clusters found in the experiments. Moreover, the sizes predicted by our model can only be taken as lower bound reference, because the presence of solute atoms within the strain field of the loops increases the microstructural features effective size, as seen by APT.

4.1. Effect of irradiation temperature

According to our model, by increasing the irradiation temperature the defect number density decreases; the mean size of SIA loops also decreases, while the size of voids increases. Consistently, an APT analysis reported in [32] suggests a lower density of NiSiPCr-clusters observed after high energy ion irradiation of the Fe-9%Cr model alloy at 420°C when compared to 300°C. Moreover, a decrease in dislocation loop density at higher irradiation temperatures was also reported in data from TEM analysis on both neutron and ion irradiated materials [33], while in-situ TEM studies on different ion-irradiated F/M model alloys revealed a similar behavior with increasing irradiation temperatures [34-37]. TEM analysis on Fe-C neutron irradiated to ~1 dpa also showed a clear tendency to progressively lower SIA loop number densities at increasing temperatures. However, their average size was concomitantly observed to increase, not decrease, especially above 350°C [38]. This means that our OKMC model correctly describes the decrease in density, but somehow fails to reproduce the expected increase in size. It is possible that this is the consequence of the hypothesis that traps (related to the presence of C atoms) are immobile in our model. In a real irradiated system C should become progressively more mobile with increasing temperature, between 250 and 350°C, and the fact that in our model this mechanism is not included may artificially reduce the effective mobility of loops, preventing defect coalescence and therefore growth. In the same neutron irradiated Fe-C alloys the density of voids is observed to decrease with increasing irradiation temperatures, while their size increases [38]: in this case our model predictions agree with both experimental trends. PAS analysis on ion irradiated Fe-Cr model alloys at 100, 300 and 420°C are also available in [33]: the second positron lifetime component was observed to have an extremely low intensity after irradiation at 420°C, meaning that the materials were almost defect free, while between 100 and 300°C the defect concentration was seen to drop by a factor two at the higher irradiation temperature, therefore

suggesting that small vacancy clusters disappear more easily at higher temperatures. Voids were also observed to form more likely at higher temperature [33], in agreement with the results of our model.

To conclude, we make an attempt at estimating the trends of irradiation hardening stemming from radiation defects versus irradiation temperature. A quantitatively correct prediction of the radiation hardening induced by the combination of the different defect populations is extremely difficult and outside the scope of this work. However, as demonstrated and discussed in [39], in a dispersed barrier model framework the increase of the yield strength due to irradiation, $\Delta\tau_{irr}$, is always *proportional* to a quantity that depends on the diameter d of the defects that hamper dislocation motion, and on the distance l between defects on the dislocation glide plane, as follows:

$$\Delta\tau_{irr} \propto \frac{1}{l}\ln\frac{2\underline{D}}{b} \tag{3}$$

Here $\underline{D}$ is the harmonic mean of d and l, $\underline{D} = \frac{dl}{d+l}$, normalized by $0.5b$ (with b=0.248 nm norm of the Burgers vector). In the case of SIA clusters d is the mean diameter reported in Fig. 1. For voids a correction factor $\pi/4$ was applied to consider an average over their spherical shape, to include dependence on where the dislocation glide plane cuts the void. In both cases, then, l is calculated as $l = \frac{1}{\sqrt{Nd}} - d$, with N the number density reported in Fig. 1. The hardening trends for all defect categories (Fig. 3) are seen to significantly decrease with the irradiation temperature. This suggests that, in terms of induced hardening, the density decrease wins over the size increase in the case of voids (see Fig. 1). The figure also suggests that a higher density of smaller SIA defects may contribute more to hardening in neutron-irradiated materials than a lower amount of bigger loops. These results are in qualitative agreement with [40], where the experimentally measured yield stress in neutron-irradiated F/M steels was seen to decrease with the irradiation temperature between 390 and 550°C: the faster diffusion of defects with temperature facilitates irradiation-induced defects to anneal out and precipitates to coarsen [40]. A similar conclusion could also be drawn from [41], where the conventional 9Cr-1Mo martensitic steel was neutron-irradiated up to 0.8 dpa in the temperature range 250–450°C: the irradiation-induced hardening was experimentally observed to rapidly decrease with increasing irradiation temperatures, this effect being enhanced above ~300°C. We can thus conclude that our nanostructure evolution model allows correct estimations in terms of hardening trends in F/M steels.

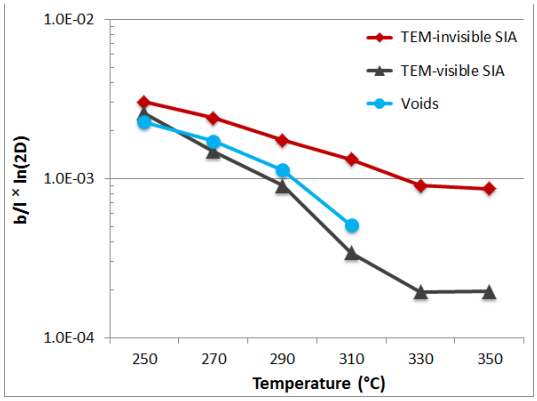

Fig. 3. Hardening trends predicted by the OKMC model, as a function of irradiation temperature.

4.2. Study on the impact of dose-rate

The dose-rate effect on the microstructural evolution and subsequent hardening under irradiation in steels is a debated issue of high importance, in connection with the use of high flux data to assess the behavior of materials at high dose, as opposite to the low flux received for long times during the operation of nuclear power plants. Neutron irradiation campaigns conducted at different dose-rates to the same dose and on the same material are both extremely expensive and difficult to run, due to a lack of appropriate irradiation facilities. The effect of dose-rate can, however, be partly assessed by comparing neutron to ion irradiation. So, here we try to compare our results with experimental data coming from the ion and neutron irradiation of the same Fe-Cr-C alloys [22,32].

The number density of SIA loops observed by TEM in ion irradiated Fe-9%Cr [32] was found to be very close to that reported for the same model material neutron irradiated at 10^{-7} dpa/s up to 0.6 dpa [22]: the remarkable increase of the SIA defects number density with the dose-rate predicted by our OKMC model was thus not observed. The number density of the small SIA cluster population representing the NiSiPCr-rich solute clusters experimentally observed in APT was seen to increase a bit under ion irradiation when compared to neutron irradiation, at 300°C [22,32], but not in a way comparable to what the simulation suggests. The experimentally observed mean size, in contrast, was found to be very close to the values predicted by our OKMC model, i.e. ~1.5 nm [32]. However, when appraising these differences in number density evolution between model and experiment, one should keep in mind that ion irradiation does not differ from neutron irradiation only because of higher dose-rates. Under ion irradiation damage is not uniformly distributed, there are gradients in defect concentrations through the thickness of the specimen because of nearby free surfaces and of the progressive slowing down of the ions, as well as a time dependence of the displacement rate (pulsed irradiation [42,43]), togeteher with possible differences in the cascade morphology and defect production efficiency [44]. Furthermore, the implanted ions can be considered as an extra source of SIAs. None of these factors have been considered in the model: taking them into account will be the goal of future work. What has been simulated here is a hypothetical neutron irradiation in the bulk at very

high flux, so high that it is in fact unattainable with neutrons. It is possible that the very moderate increase in density between neutron and ion irradiation experiments comes from the fact that in the latter case several loops are eliminated through the surface, or that the existence of a gradient in the concentration of defects leads to an averaging through the thickness. A second hypothesis might be that what leads to an overestimation of the density of loops in our model is the treatment of traps, which are assumed to be present since the very beginning while in reality they should be created during the irradiation process, in the form of complexes between carbon atoms and vacancies. When the dose-rate is very high, there may be no time for all vacancies to end up attached to carbon atoms: this means that the model may be overestimating the number of traps and thus excessively limit the mobility of SIA clusters. At the same time, TEM analysis on Fe-Cr alloys ion irradiated at two different dose-rates during different irradiation campaigns did show an increase in the SIA cluster population number density with increasing irradiation flux [45]. This suggests that, when all other variables take the same value, an increase of dose rate does lead to higher densities. The average diameters of TEM-visible loops, on the other hand, were reported to be about 6.5 nm at ~0.3 dpa and not to increase significantly with the dose-rate [45]. Moreover, the number density of Cr-enriched regions identified by APT was found to be just below the dislocation loop density measured by TEM [45]: this suggests once more that these features may indeed be associated with small dislocation loops and that at high dose rate the density of the population of invisible and visible SIA clusters tends to coincide, as also predicted by our model.

5. Conclusions

The OKMC model developed in [8] allowed us to make some considerations on the nanostructural evolution of neutron irradiated F/M model alloys under different conditions of temperature and dose-rate. However, the lack of experimental data on materials neutron irradiated under otherwise similar conditions at different temperatures and dose-rates did not allow a full validation of our results and globally in this work only tendencies could be analysed and compared. While some of the trends predicted by the model are clearly correct, others suggest that some of the simplifying assumptions made in it, especially concerning the immobility of traps for SIA clusters and their presence since the very beginning of the irradiation, might not be fully adequate to account precisely for the effect of temperature and dose-rate. Yet, the model has the advantage of providing insight concerning the origin of the effects observed, potentially providing clues about how to mitigate them. Within the limitations stated, a significant reduction in both number density and mean size of the SIA cluster population could be observed only above ~290°C, as a consequence of the enhanced mobility of defect clusters with temperature and therefore increased absorption at sinks. Number density and mean size are assumed to control hardening and embrittlement of materials subjected to neutron irradiation. As a result, the model allows trends consistent with the experimentally observed progressive disappearance of irradiation hardening and embrittlement to be found, when the irradiation temperature increases between 300 and 400°C [5,40]. At the same time, high fluxes were seen to create a much higher density of SIA clusters, partly identifiable with the small NiSiPCr-rich solute cluster population experimentally observed in APT: since their average size was also predicted to slightly increase with the irradiation flux, the combination of these two effects suggest a (moderate) increase of the hardening with increasing irradiation fluxes.

Acknowledgements

This work has been carried out within the framework of the EUROfusion Consortium and has received partial funding from the Euratom research and training programme 2014-2018 under grant agreement No 633053. The research leading to these results was also partly funded by the Euratom's Seventh Framework Programme FP7/2007-2013 under grant agreement No. 604862 (MatISSE project) and contributes to the EERA (European Energy Research Alliance) Joint Programme on Nuclear Materials (JPNM). The views and opinions expressed herein do not necessarily reflect those of the European Commission.

References

[1] H. Tanigawa et al., J. Nucl. Mater. 417 (2011) 9.
[2] T.R. Allen et al., JOM 60 (2008) 15.
[3] Yeong-il Kim et al., Sci. Technol. Nucl. Ins. Vol. 2013 (2013) 290362 (18 pages).
[4] D.S. Gelles, J. Nucl. Mater. A 293 (1996) p.233.
[5] R.L. Klueh and D.R. Harries, High Chromium Ferritic and Martensitic Steels for Nuclear Applications, ASTM, West Conshohocken, PA, 2001.
[6] K. Ehrlich, Fusion Engng Des. 71 (2001) p.56.
[7] A. Kohyama et al., J. Nucl. Mater. 233-237 (1996) 138.
[8] M. Chiapetto, L. Malerba, C.S. Becquart, J. Nucl. Mater. 465 (2015) 326–336.
[9] M. Lambrecht, PhD thesis, University of Gent, 2009.
[10] C. Domain, C. Becquart, L. Malerba, J. Nucl. Mater. 335 (2004) 121–145.
[11] V. Jansson, M. Chiapetto, L. Malerba, J. Nucl. Mater. 442 (2013) 341–349.
[12] V. Jansson, L. Malerba, J. Nucl. Mater. 443 (2013) 274–285.
[13] A.B. Bortz, M.H. Kalos, J.L. Lebowitz, J. Comput. Phys. 17, (1975) 10–18.
[14] W. Young, E. Elcock, Proc. of the Physical Society 89 (1966) 735.
[15] R. Stoller, J. Nucl. Mater. 233 (1996) 999–1003.
[16] R. Stoller, G. Odette, B.Wirth, J. Nucl. Mater. 251 (1997) 49–60.
[17] R. Stoller, A. Calder, J. Nucl. Mater. 283 (2000) 746–752.
[18] T. Karthikeyan, M.K. Dash, S. Saroja, M. Vijayalakshmi, Micron 68 (2015) 77–90.
[19] C. Domain, C. Becquart, L. Malerba, in: N. Ghoniem (Ed.), Proc. of Second International Conference on Multiscale Materials Modeling: October 11–15, 2004, Los Angeles, California, Mechanical and Aerospace Engineering Department, University of Calif., 2004.
[20] M. Matijasevic, A. Almazouzi, J. Nucl. Mater. 377 (2008) 147–154.
[21] F. Nichols, J. Nucl. Mater. 75 (1978) 32–41.
[22] M. Hernández Mayoral et al., Deliverable D4.9 (Public), GETMAT Project, Grant Agreement N°: FP7-2121175 (2013).
[23] M. Hernández-Mayoral, D. Gómez-Briceño, J. Nucl. Mater. 399 (2010) 146–153.
[24] M. Hernández-Mayoral, C. Heintze, E. Oñorbe, Submitted to J. Nucl. Mater. (2014).
[25] E.E. Zhurkin, D. Terentyev, M. Hou, L. Malerba, G. Bonny, J. Nucl. Mater. 417 (2011) 1082.
[26] L. Malerba, C.S. Becquart, C. Domain, J. Nucl. Mater. 360 (2007) 159–169.

[27] V. Kuksenko, C. Pareige, P. Pareige, J. Nucl. Mater. 432 (2013) 160.
[28] E.E. Zhurkin, D. Terentyev, M. Hou, L. Malerba, G. Bonny, J. Nucl. Mater. 417 (2011) 1082.
[29] G. Bonny, D. Terentyev, E.E. Zhurkin, L. Malerba, J. Nucl. Mater. 452 (2014) 486.
[30] I.M. Neklyudov, V.N. Voyevodin, J. Nucl. Mater. 212 (1994) 39.
[31] Z. Jiao, G.S. Was, Acta Mater. 59 (2011) 4467.
[32] M. Hernández Mayoral et al., Deliverable D4.7 (Public), GETMAT Project, Grant Agreement N°: FP7-212175 (2013).
[33] T. Muroga, H. Watanabe, N. Yoshida, J. Nucl. Mater. 174 (1990) 282–288.
[34] Z. Yao, M. Hernández-Mayoral, M.L. Jenkins, M.A. Kirk, Philos. Mag. Vol. 88, No. 21 (2008) 2851-2880.
[35] M. Hernandez-Mayoral, Z. Yao, M.L. Jenkins, M.A. Kirk, Philos. Mag. 88 (2008) 2881.
[36] Z. Yao, M.L. Jenkins, M. Hernández-Mayoral, M.A. Kirk, Philos. Mag. (2010) 1–12.
[37] M.L.Jenkins, Z.Yao, M.Hernández-Mayoral, M.A.Kirk, J. Nucl. Mater. 389 (2009) 197–202.
[38] L.L. Horton, J. Bentley, K. Farrell, J. Nucl. Mater. 108&109 (1982) 222–233.
[39] G. Monnet, Acta Mater. 95 (2015) 302–311.
[40] R.L. Klueh, K. Shiba, M.A. Sokolov, J. Nucl. Mater. 377 (2008) 427–437.
[41] A. Alamo et al., J. Nucl. Mater. 283–287 (2000) 353–357.
[42] E.P. Simonen, N.M. Ghoniem, N.H. Packan, J. Nucl. Mater. 122 & 123 (1984) 391–401.
[43] E.H. Lee, N.H. Packan, L.K. Mansur, J. Nucl. Mater. 117 (1983) 123.
[44] G.S. Was, Fundamentals of Radiation Materials Science: Metals and Alloys, Springer (2007), p. 571.
[45] C.D. Hardie, C.A. Williams, S. Xu, S.G. Roberts, J. Nucl. Mater. 439 (2013) 33–40.